Interplay between Amphiphilic Stabilizers and Cholesterol in the Stabilization of Itraconazole Nanoparticles Prepared by Flash Nanoprecipitation

Ka Yee Wan[1], Si Nga Wong[2], Ka Wai Wong[3], Shing Fung Chow[2,*], Albert Hee Lum Chow[1,*#]

[1]School of Pharmacy, The Chinese University of Hong Kong, Sha Tin, Hong Kong
[2]Department of Pharmacology and Pharmacy, The University of Hong Kong, Pokfulam, Hong Kong
[3]Genvida (HK) Company Limited, Hong Kong

* *Corresponding authors*

Shing Fung Chow
Department of Pharmacology and Pharmacy
Li Ka Shing Faculty of Medicine
The University of Hong Kong
L2-08B, Laboratory Block,
21 Sassoon Road, Pokfulam, Hong Kong
Email: asfchow@hku.hk
Tel: 852 39179026
Fax: 852 28170859

Albert H. L. Chow
School of Pharmacy
The Chinese University of Hong Kong,
8/F, Lo Kwee-Seong Integrated
Biomedical Sciences Building, Area 39,
Shatin, N.T., Hong Kong
Email: albert-chow@cuhk.edu.hk
Tel: 852 26096829
Fax: 852 26035295

#Present address:

Aptorum Pharmaceutical Development Limited, Unit 232, 2/F, Building 12W, Hong Kong Science and Technology Park, Shatin, N.T., Hong Kong

E-mail: albert.chow@aptorumgroup.com; Tel: 852 36119401; Fax: 852 35905690

ABSTRACT:

While flash nanoprecipitation (FNP) has proven to be an extremely rapid and highly efficient nanoparticle fabrication process for hydrophobic drugs, physical instability associated with non-equilibrium molecular orientation of amphiphilic stabilizers (ASs) in nanoparticles remains a major snag in the general application of this nanotechnology, particularly for a drug with ACDLogP in the range of ~2 to ~9. This study was aimed at elucidating the co-stabilizing role of cholesterol (CLT) in the FNP of AS-stabilized nanoparticles of itraconazole (ITZ), a model drug with ACDlog P of 4.35±1.22. The presence of CLT was shown to reduce the initial particle size and markedly improve the physical stability of ITZ nanoparticles during short-term storage. The stability-enhancement by CLT can be linked to its higher miscibility or stronger interaction with the AS hydrophobic moiety than with ITZ (as reflected by the absolute differences of their solubility parameter values). Surface analyses employing X-ray photoelectron spectroscopy (XPS) and atomic force microscopy (AFM) suggest that, through the co-precipitation of CLT with ITZ to form a mixed hydrophobic drug core, the CLT molecules that are exposed on the core surface serve to afford a stronger and more timely surface anchorage of the AS hydrophobic moieties, thereby facilitating the rearrangement of AS molecules towards the stable micelle-like structure. The present findings offer important insight into the mechanistic interplay between amphiphilic stabilizer and co-stabilizer in enhancing the physical stability of drug nanoparticles, and may carry important implications for the development of more stable and efficacious nanoparticle therapeutics.

Keywords: flash nanoprecipitation; itraconazole nanoparticles; amphiphilic stabilizers; cholesterol; solubility parameter; physical stability

1. Introduction

Formulating poorly water-soluble drugs as nanoparticles represents an attractive drug delivery option. Not only the solubility, but also the bioavailability of such drugs can be enhanced with this formulation approach, as substantiated in *in vivo* studies employing various routes of drug administration including the oral [1], parenteral [2], and pulmonary routes [3]. With tight control of their particle size (generally less than 200 nm), surface properties and stability, nanoparticles can even bypass first-pass metabolism [4], display enhanced permeability and retention (EPR) effect in tumor targeting [5] and penetrate restrictive biological barriers [6].

With the rapid advancement in nanoparticle technology, a growing number of nanoparticle fabrication methods have emerged, among which the antisolvent precipitation process, flash nanoprecipitation (FNP), has attracted considerable attention, mainly due to its general applicability to hydrophobic drugs as well as its ease, good controllability, and high efficiency of operation. FNP utilizes smartly designed mixers such as confined impinging jet mixer (CIJM) and multi-inlet vortex mixer (MIVM) to achieve extremely rapid and homogeneous mixing of the solution and antisolvent streams prior to nanoparticle precipitation [7-9]. The technology has been widely demonstrated to possess the capability of reproducibly fabricating drug nanoparticles having particle size less than 200 nm with the aid of amphiphilic stabilizers (ASs) [10-11].

Despite the excellent reproducibility of FNP in nanoparticle generation, attempts to develop stable drug nanoparticle suspensions (nanosuspensions) using this technology have met with limited success [12-14]. The major snag with FNP is that it tends to yield unstable nanosuspensions for organic compounds or drugs with ACDLogP in the range of ~2 to ~9 [15], which has commonly been ascribed to Ostwald ripening [16] and non-equilibrium molecular orientation of AS in the nanoparticles [17]. This instability issue has severely stifled the general utility of FNP for production of drug nanosuspensions since the majority of drugs fall within such ACD log P range. While the effect of Ostwald ripening can be suppressed by removing residual organic solvent from the nanosuspensions via dialysis [18], the non-equilibrium molecular orientation of ASs, particularly those with large molecular mass or long molecular chains, remains a formidable hurdle that has yet to be overcome. Our previous work on the production of AS-stabilized nanoparticles of itraconazole (ITZ), a model drug with ACDLog P of 4.35

±1.22, by FNP demonstrated that the latter phenomenon occurred in both freshly generated blank AS and AS-stabilized ITZ (ITZ-AS) nanoparticles [20]. For the blank AS nanoparticles, AS molecules have been shown to undergo fairly rapid self-assembly into a micellar structure during storage. In contrast, for the ITZ-AS nanoparticles with ITZ forming the core, the AS molecules rearranged slowly towards or even away from the micelle-like configuration, depending on whether they could timely and firmly anchor with their hydrophobic moieties on the inner drug core, which probably explains why particle growth and aggregation cannot be entirely suppressed.

As a strategy to circumvent the aforementioned stability problem, we propose to incorporate the co-stabilizer, cholesterol (CLT; ACDLogP = 9.85±0.28), into the drug core of the ITZ-AS nanoparticles, so that the AS molecules can be more timely and firmly attached to the hydrophobic drug core via their hydrophobic tails to facilitate the orientation of their hydrophilic heads towards the external aqueous phase. The latter process is particularly critical for achieving long-term storage stability for the nanoparticles. We reckon that in the presence of a hydrophobic co-stabilizer, the co-stabilizer and hydrophobic drug will most likely form a mixed particle core together with a certain amount of co-stabilizer being exposed on the core surface. Such surface-exposed co-stabilizer can then serve to strengthen the interaction between the hydrophobic particle core and the AS hydrophobic tails. We hypothesize that if the solubility parameter value of the co-stabilizer ($\delta_{co-stabilizer}$) is closer to that of the hydrophobic tail of AS than to that of the co-precipitating drug, a higher affinity will exist between the co-stabilizer and AS than between the drug and AS, giving rise to the formation of more stable nanoparticles. To verify this hypothesis, we have reformulated the ITZ-AS nanoparticles with the addition of CLT as co-stabilizer, and have characterized the reformulated nanoparticles using essentially the same techniques as previously described for the formulation without CLT [20]. The reason for using basically the same study approach here was to allow direct comparison of results between the CLT-incorporated and CLT-free nanoparticle formulations. As implicitly stated in our hypothesis, the choice of CLT in the present study was based on its similarity in solubility parameter value to the hydrophobic moieties of the ASs employed. The solubility parameter (δ_{CLT}) value of CLT is 19.5 $(MJ/m^3)^{1/2}$ [21], which is more comparable to those of vitamin E succinate [19.0 $(MJ/m^3)^{1/2}$] (calculated using the method of Hoy [19]) in TPGS and of PLA [~21.3 $(MJ/m^3)^{1/2}$] [17] in PEG-PLA than to that

of ITZ [26.5 $(MJ/m^3)^{1/2}$] [22]. In addition, CLT is one of the most abundant endogenous lipids in human body, which is essential for building up and regulating cell membranes. CLT has also been widely exploited as an excipient in drug formulation not only due to its established safety profile and relatively low cost, but also to its potential capability in facilitating cellular drug uptake. The high cellular affinity of CLT has been supported by the study of Hwang et al, in which a larger number of cells were seen to adhere to the layers containing synthesized diblock molecules of CLT and PLA than to a PLA control surface [23]. It is also worth noting that CLT is commonly used in liposome formulations for stability enhancement. However, the stabilization mechanism of CLT in liposomes cannot be equated with that in nanoparticles generated by FNP. Thermodynamic equilibrium molecular orientation (i.e., AS with all hydrophilic heads pointing to the surrounding aqueous medium and all hydrophobic tails directing towards immiscible organic solvent core) exists when liposomes are formed initially. Instability of liposomes is generally caused by the high molecular mobility and desorption of the AS. The inclusion of CLT favors the stabilization of liposomes by reducing the desorption of AS through positioning of the CLT between the hydrophobic tails of AS to decrease the mobility of AS [24-25]. In contrast, the observed instability of ITZ-AS nanoparticles generated by FNP was induced by non-equilibrium molecular orientation rather than desorption of AS. This has been substantiated by our previous study, which demonstrated that PEG-PLA 2k-10k, which exhibited very limited desorption from the ITZ particle core, yielded the most unstable ITZ-AS nanoparticles [20].

2. Materials and methods

2.1.Materials

Itraconazole (ITZ), ketoconazole (KTZ) and terconazole (TZ) with purity > 99% were supplied by Yick-Vic Chemicals & Pharmaceuticals Ltd. (Hong Kong, China). D-α-tocopheryl polyethylene glycol 1000 succinate (TPGS), cholesterol (CLT) and ammonium acetate were purchased from Sigma Aldrich (USA). Di-block copolymers poly(ethylene glycol)-b-poly(DL-lactide) (PEG-PLA) of molecular weight ratios of 2k-2k, 2k-10k and 5k-10k were obtained from SRI Biomaterials Inc. (California, USA). Dimethylformamide (DMF) and tetrahydrofuran (THF) of analytical grade were received from RCI Labscan Limited. Acetonitrile (ACN) of

HPLC grade and acetic acid of analytical grade were supplied by Duksan Pure Chemicals (Korea) and BDH Laboratory Supplies (UK) respectively. Deionized water with a final resistivity not less than 18.0 MΩ·cm was generated by a Millipore Direct-QTM water purification system (USA).

2.2.Preparation of ITZ nanoparticles

ITZ nanoparticles in suspension form (i.e., ITZ nanosuspensions) were prepared by FNP using a four-stream multi-inlet vortex mixer (MIVM) as described previously [20]. The detailed geometry and dimension of the mixer can be found elsewhere [8]. One stream (inlet 1) consisted of an organic solvent (DMF) with ITZ (5 mg/ml), AS (5 mg/ml) and/or CLT (1-5 mg/ml) while the other three streams (inlets 2, 3 and 4) contained deionized water serving as an antisolvent. The ASs used were TPGS and PEG-PLAs of molecular weights of 2k-2k, 2k-10k and 5k-10k. The flowrates of different streams were precisely controlled by means of two digital programmable syringe pumps (Harvard Apparatus, PHD 2000, infusion only model, USA). The flowrates of Inlets 1 and 3 were both set at 11 ml/min while those of Inlets 2 and 4 at 99 ml/min. The ITZ nanosuspension was collected at the exit port of the MIVM. As before, the dimensionless Reynold number (Re), which is conventionally used to depict fluid flow condition, was fixed at ~4,200 throughout the experiment. Below is the mathematical expression of Re:

$$Re = \sum_{i=1}^{4} \frac{\rho_i v_i D}{\mu_i} = \frac{4}{\pi D} \sum_{i=1}^{4} \frac{\rho_i Q_i}{\mu_i} \qquad \text{Eq. 1}$$

where i is the stream number, ρ is the fluid density (kg/m^3); D is the characteristic diameter of the MIVM; v is the stream velocity (m/s); μ is the fluid viscosity (Pa·s) and Q is the stream flowrate (m^3/s).

2.3.Particle size and zeta potential measurements

Intensity-weighted particle size, ~~particle size,~~ polydispersity index (PI) and zeta potential of nanoparticles were measured using a Delsa™ Nano C analyzer (Beckman Coulter, Inc., USA) as previously described [20]. The time courses of particle size measurements would be terminated if visual flocculates were observed or if the measured particle size was larger than 1,000 nm.

2.4.High performance liquid chromatography (HPLC)

Assay of ITZ employed a Waters Alliance 2695 HPLC system coupled with a Waters 996 photodiode array detector (Waters Corporation., USA) and a C_{18} column (Symmetry®, 5 µm, 4.6 mm × 150 mm I.D., Waters Corporation, USA). The mobile phase, consisting of acetonitrile/10mM ammonium acetate solution and acetic acid (pH~5.7) in a volumetric ratio of 3:2, was eluted isocratically at 1 ml/min. The detection wavelength was set at 261 nm, and the injection volume was 10 µl. The retention time of ITZ was ~10 min.

2.5.Determination of drug loading and drug encapsulation efficiency

Determination of drug loading (drug mass percentage) and drug encapsulation efficiency of nanosuspensions involving ultrafiltration through an Amicon® Ultra 30K centrifugal filter device (Millipore Corporation, Billerica, MA, USA) followed the same protocols as previously reported [20]. To estimate the extent of AS desorption from nanoparticles, drug mass percentage of nanosuspension without ultrafiltration was also determined and compared with that obtained for the nanosuspension with ultrafiltration (i.e. drug loading). The former would be smaller than the latter if the extent of AS desorption from the nanoparticle surface was high and the free drug concentration in suspending medium was negligibly low.

2.6.Surface composition

Surface elemental composition of nanoparticles was determined using X-ray photoelectron spectroscopy (XPS) as described previously [20]. In brief, XPS spectrum was collected using a Shimadu Kratos Axis Ultra DLD multi-technique surface analysis system (Japan) with a monochromatized Al K-α X-ray (hv 1486.6eV) source. Passing energy was 40eV and the angle of X-ray was 90^{o}. Peak deconvolution of C1s envelope was conducted using XPSpeak (version 4.1) software with reference to the National Institute of Standards and Technology (NIST) XPS database (version 4.1; http://srdata.nist.gov/xps) and Handbook of X-ray and Ultraviolet Photoelectron Spectroscopy [26].

2.7.Surface morphology and phase imaging

A Tapping Mode™ atomic force microscope (TM-AFM, Dimension 3100, Digital Instruments, USA) was employed to capture the AFM and phase images of nanoparticles. Sample was gently sprayed onto a glass wafer and air dried prior to analysis. Spring constant, resonance frequency and cantilever length were set at 40 N/m, 300 kHz, and 125 µm, respectively. The set-point ratio was 0.6-0.9.

2.8.Fourier-transform infrared (FTIR) spectroscopy

Sample and potassium bromide (KBr) in a mass ratio of ~1:30 were gently triturated using a marble mortar and pestle. A thin disc was made by compressing the solid mixture under 8 tons force using a hydraulic press. The disc was scanned over the ranges of 1500-4000 cm^{-1} at an interval of 2 cm^{-1} using a Spectrum BX FTIR spectrophotometer (PerkinElmer Inc., USA).

2.9. Statistical analysis

All characterization tests and measurements were performed in triplicate with separate batches of samples (i.e. three independent FNP runs per formulation). Unpaired Student's t-test was used to analyze the collected data. A p-value less than 0.05 was considered as significant.

3. Results and discussion

3.1. Particle size and stability of ITZ-AS nanoparticles with addition of CLT

To examine the stability-enhancing effects of CLT on various ITZ-AS nanoparticles, part of the stability data obtained previously for the CLT-free nanoparticle formulations [20] is reproduced here for direct comparison with those of the CLT-containing nanoparticles in the present study. As different chemical structure of ASs can affect the resulting hydrophobic interaction and structure-dependent re-orientation of ASs on particle stability, various block length of PEG-PLAs (2k-2k; 2k-10k; 5k-10k) beside TPGS were included to study the influence of molecular size of AS.

In Fig. 1, it can be seen that inclusion of CLT in various nanoparticle formulations containing equivalent amounts of ITZ and AS generally reduced the initial particle size. The size reduction effect was most apparent for the samples with PEG-PLAs as stabilizers. For instance, the initial particle size of the ITZ-PEG-PLA 2k-10k

nanoparticle sample decreased substantially from 126.1 ± 3.6 nm to 94.8 ± 3.0 nm ($p = 0.00038$) when CLT was added in one-fifth the amount of ITZ to the formulation (i.e., ITZ:AS:CLT = 1:1:0.2 w/w/w). Being hydrophobic, CLT would tend to be co-encapsulated with ITZ in the particle core to minimize the high solid-water interfacial energy upon precipitation, suggesting that the initial particle size depended on the surface properties of the particle core.

The presence of CLT also alleviated the instability of ITZ-AS nanoparticles stored at room temperature, as shown in Fig. 2. For example, the increase in particle size of nanoparticles after two hours of storage at room temperature was significantly smaller ($p = 0.013$) for the ITZ-TPGS nanoparticles with CLT [ITZ:TPGS:CLT = 1:1:0.2 w/w/w, increased by 12.1±1.0% (from 88.4±1.8nm to 99.1±1.6nm)] than for those without CLT [ITZ:TPGS = 1:1 w/w, increased by 87.6±15.4% (from 91.1±5.9nm to 170.2±3.2nm). Similar stability enhancement was also observed for the samples stored under refrigerated condition (Fig. 3), indicating that temperature does not mediate the stability-enhancing effect of CLT on the nanoparticles.

3.2. Optimal concentration of CLT for nanoparticle stability enhancement

The data for the formulations employing PEG-PLA 2k-2k and PEG-PLA 2k-10k in Fig. 1 suggest that when used in excess, CLT could undesirably increase the initial particle size of ITZ-AS nanoparticles, as the increased amount of CLT would also be counted into the final particle size. During short-term storage (2 h), an increase in the relative mass concentration of CLT (ITZ:AS:CLT from 1:1:0.2 to 1:1:1) in the formulation resulted in similar particle sizes at 2h for nanoparticles containing PEG-PLA 2k-2k (182.9±1.97nm and 180.7±0.95nm for the ITZ:AS:CLT ratio of 1:1:0.2 and 1:1:1 respectively; p=0.18) and PEG-PLA 5k-10k (160.57±5.73nm and 156.60±6.20nm for the ITZ:AS:CLT ratio of 1:1:0.2 and 1:1:1 respectively; p=0.46), but larger particle sizes at 2h in the cases of PEG-PLA 2k-10k (154.57±1.11nm and 169.60±3.49nm for the ITZ:AS:CLT ratio of 1:1:0.2 and 1:1:1 respectively; p=0.011) and TPGS (99.10±1.56nm and 114.27±1.43nm for the ITZ:AS:CLT ratio of 1:1:0.2 and 1:1:1 respectively; p=0.00025) (Fig. 2). This observation is perhaps not unexpected as the added amount of CLT in ITZ hydrophobic core will also require protection from AS. Larger amount of AS is generally required to stabilize more amount of CLT. With fixed amount of AS and increased amount of CLT, further growth of particles would result as

lower particle surface to volume ratio allows stabilization with the less AS. The nanoparticles optimized for both initial particle size and physical stability should be the formulation with the minimal amount of CLT required to enhance particle stability without adversely altering the particle size. Avoidance of using more than the required amount of CLT in the formulation is also important for maximizing drug loading without compromising particle stability. Thus subsequent studies in this work employed formulations containing ITZ and CLT in the mass ratio of 1:0.2 to further probe into the role of CLT in nanoparticle formation and stabilization.

3.3. Stabilization mechanism of CLT in ITZ-AS nanoparticles

As shown in a previous study, nanoparticles hold electrical repulsive force for preventing aggregation only if they display a sufficiently large zeta potential, i.e., absolute magnitude of zeta potential > 30 mV [27]. All the nanoparticle formulations containing AS and CLT exhibited a zeta potential of less than 30 mV in magnitude, suggesting that the incorporated CLT exerted no significant impact on the surface charges of the nanoparticles (see Fig. S1 in supplementary information). This is consistent with non-electrolytic nature of CLT. Hence, particle stability mainly depends on the hydrophilic groups present on the particle surface to maintain particle dispersion in aqueous suspending medium as well as to prevent particle aggregation through steric hindrance.

To investigate whether CLT would induce Ostwald ripening and/or desorption of AS, the concentration of free drug as well as change in drug mass percentage in the nanosuspensions with CLT before and after ultrafiltration were determined. If Ostwald ripening and/or desorption of AS did occur, it would be most obvious with the ITZ-TPGS-CLT nanoparticles since TPGS has the highest aqueous solubility and molecular mobility. Using this nanoparticle sample for illustration purpose, it was demonstrated that the measured drug loading in ITZ-TPGS-CLT nanoparticles (45.2% ± 0.18%) was in close agreement with the theoretical estimate (45%) and with the drug mass percentage of ITZ-TPGS-CLT nanosuspension without ultrafiltration (45.1% ± 0.42%). In addition, the drug encapsulation efficiency was found to be larger than 99%, indicating that the amount of free drug present was negligible. All these observations suggest that neither Ostwald ripening nor desorption of TPGS from particle surface is involved in the stability of the ITZ-TPGS-CLT nanoparticles. Consequently, CLT exerts

its stability-enhancing effect on ITZ-AS nanoparticles probably via the rearrangement process of AS molecules in the nanoparticles (see also later discussion).

3.4. Interaction between AS and surface of particle core

As established earlier, addition of CLT generally afforded smaller ITZ-AS nanoparticles when freshly formed. Interestingly, for the ITZ nanoparticles stabilized by the various PEG-PLAs (i.e. 2k-2k, 2k-10k, 5k-10k), the initial particle sizes were nearly identical and independent of the molecular weight of the PEG-PLA (Fig. 4). It is possible that the co-existence of CLT with ITZ in the particle core had resulted in equally strong and uniform interaction with all the three PEG-PLAs whose effects on initial particle size were thus not readily differentiable. It also implies that the surface properties of the particle cores of these samples were similar.

For the PEG-PLA-protected ITZ nanoparticles without CLT, the short-term stability (2 h) increased with an increase in length of hydrophilic PEG [the particle size was increased by 120.64±11.96% and 91.93±12.64% for PEG-PLA 2k-10k and PEG-PLA 5k-10k respectively; $p = 0.046$] but decreased with an increase in length of hydrophobic PLA (the particle size was increased by 79.77±3.28% and 120.64±11.96% for PEG-PLA 2k-2k and PEG-PLA 2k-10k respectively; $p = 0.021$) [20]. However, after incorporation of CLT (Fig. 4), the short-term stability of ITZ nanoparticles with the PEG-PLAs exhibiting different PEG lengths became similar (the particle size was increased by 63.16±5.67% and 57.75±10.56% for PEG-PLA 2k-10k and PEG-PLA 5k-10k respectively; $p = 0.49$) whereas the stability appeared better with the PEG-PLA of longer PLA (the particle size was increased by 92.20±9.31% and 63.16±5.67% for PEG:PLA 2k-2k and PEG-PLA 2k-10k respectively; $p = 0.015$). It should be noted that due to its predominantly hydrophobic nature, CLT alone cannot serve as a primary stabilizer for the ITZ nanoparticles (as attested by formation of visible precipitates in seconds after FNP), and AS is always required for complete coverage of both ITZ and CLT to achieve the desired stability. In other words, direct protection of the nanoparticles is only offered by the AS (PEG-PLA in this case). It is possible that CLT present on the surface of ITZ-CLT core, being closer than ITZ to PLA in terms of intermolecular interactions, reinforces the hydrophobic binding of the core with the PLA tails of PEG-PLA, thereby providing firm anchorage of the latter on the core while allowing the PEG heads to re-orientate readily to the external aqueous medium. As

alluded to earlier, the miscibility or interaction strength among CLT, ITZ and hydrophobic moiety of the AS can be deduced from the absolute differences in their solubility parameter values. Since the solubility parameter (δ) values of CLT, ITZ and PLA are 19.5, 26.5, and 21.3 $(MJ/m^3)^{1/2}$ respectively, the absolute difference in solubility parameter value between CLT and PLA ($|\delta_{CLT} - \delta_{PLA}|$) would be 1.8 $(MJ/m^3)^{1/2}$, which is much smaller than that between ITZ and PLA [$|\delta_{ITZ} - \delta_{PLA}|$=5.2 $(MJ/m^3)^{1/2}$], suggesting that CLT has a higher miscibility or stronger interaction with PLA than with ITZ. Similar argument can be applied to the case with TPGS as the primary stabilizer where $|\delta_{CLT} - \delta_{vitamin\ E\ succinate}|$=0.5 $(MJ/m^3)^{1/2}$, which is also considerably lower than $|\delta_{ITZ} - \delta_{vitamin\ E\ succinate}|$=7.5 $(MJ/m^3)^{1/2}$. In principle, the stronger the interaction between the hydrophobic tails of the AS and particle core, the easier the orientation of the hydrophilic heads towards the external aqueous phase.

3.5. Surface analysis of ITZ-AS-CLT nanoparticles

To investigate the effect of CLT on initial particle surface composition and molecular rearrangement of ASs, the most stable ITZ-TPGS-CLT nanoparticle formulation (ITZ:TPGS:CLT = 1:1:0.2 w/w/w; see Fig. 4) was further analyzed for its surface composition, morphology and phase image. Essentially the same quantitative XPS approach as previously described for the CLT-free nanoparticle formulation [20] was employed here to monitor the change in surface composition of the CLT-added ITZ-AS nanoparticles as a function of storage time.

The peaks of all carbon species of interest can be categorized into three binding energy ranges: (i) $C_{(285)}$ (BE = 285.0eV), (ii) $C_{(286\text{-}288)}$ (BE = 286 - 288eV) and (iii) $C_{(288\text{-}290)}$ (BE = 288 - 290eV) (see Fig. S2 in supplementary information). Fig. 5 displays the relative atomic concentrations of all components on the particle surface of ITZ nanoparticles. It is noted that chlorine (Cl) element is excluded in the analysis owing to its relatively small atomic composition in ITZ and thus weak signal. In theoretical model, uniform distribution and an absence of preferred orientation of all interested chemical species are proposed for the structure of the nanoparticles. That is, the particle surface coverage is contributed uniformly by all species. $C_{(286\text{-}288)}$ peaks of TPGS and CLT overlap with one another and are, therefore, not amenable to peak deconvolution. Owing to the fact that the hydrophobic part of CLT is solely contributed by $C_{(285)}$, $C_{(285)}$ was included to serve as a reference tracer for comparison although ITZ and the

hydrophobic part of TPGS also contribute to $C_{(285)}$, and $C_{(285)}$ may not be sufficiently precise due to possible adsorption of a small amount of environmental carbon [28]. For the freshly prepared ITZ-CLT nanoparticles without TPGS, the experimental relative atomic concentration of $C_{(285)}$, $C_{(288\text{-}290)}$ of ITZ and $C_{(286\text{-}288)}$ of hydrophilic part of CLT (96.16±2.03%, 3.18±1.61% and 0.66±0.42%) were close to its theoretical value (93.40%, 5.58% and 1.02%). The higher experimental $C_{(285)}$ compared with the theoretical one may be due to adsorption of environmental carbon. Since the theoretical value was calculated based on the assumption of homogenous mixture of ITZ and CLT, it can be deducted that the freshly prepared ITZ-CLT core was nearly homogenous mixture. This is not surprising as the precipitation time of FNP process is extremely short, so ITZ and CLT have no sufficient time to have preferred orientation and arrangement. Additionally, the relative atomic concentration of $C_{(286\text{-}288)}$ for the hydrophilic part of CLT was extremely low (0.66 ± 0.42%). This explains why coarse precipitates were observed within seconds right after production of ITZ-CLT nanoparticles (i.e., extremely unstable). Therefore, TPGS must be present mainly on the particle surface to stabilize ITZ-TPGS and ITZ-TPGS-CLT nanoparticles. This was further substantiated by the observation that the relative atomic concentration of $C_{(285)}$ of freshly produced ITZ-TPGS-CLT nanoparticles (55.82 ± 1.49%) was considerably closer to that of ITZ-TPGS nanoparticles (67.22 ± 1.46%) than that of ITZ-CLT nanoparticles (96.16 ± 2.03%).

Fig. 6a-c show the relative atomic concentration ratios of the hydrophilic part of AS and CLT to the hydrophobic part of AS ($R_{Hc:L}$), the relative atomic concentration ratio of ITZ to the hydrophilic part of AS and CLT plus the hydrophobic part of AS ($R_{D:Hc+L}$), and the relative atomic concentration ratio of the hydrophilic part of AS and CLT to ITZ plus the hydrophobic part of AS ($R_{Hc:D+L}$) on the surface of nanoparticles, respectively. The theoretical estimates of $R_{Hc:L}$, $R_{D:Hc+L}$ and $R_{Hc:D+L}$ of the ITZ-TPGS formulations with and without CLT were similar since the amount of CLT added was relatively small (ITZ:TPGS:CLT = 1:1:0.2 w/w/w). Comparing the different nanoparticle samples right after production, $R_{D:Hc+L}$ of the nanoparticles with CLT (0.035±0.0054) was much smaller ($p = 0.00018$) than that of the sample without CLT (0.104±0.0032), suggesting that the addition of CLT led to a smaller portion of drug being exposed to the aqueous medium. As TPGS is critical for stabilizing nanoparticles, and the ITZ-TPGS-CLT nanoparticles are more stable than the ITZ-TPGS nanoparticles,

the ITZ-TPGS-CLT nanoparticles are probably coated by more TPGS compared with the ITZ-TPGS nanoparticles. The improved adsorption of TPGS in ITZ-TPGS-CLT nanoparticles is probably attributable to a favourable modification of the surface properties of the hydrophobic core by CLT. In addition to enhancing the adsorption of TPGS, CLT can also facilitate the re-orientation of the hydrophobic part of TPGS towards the hydrophobic core through enhanced hydrophobic interaction, resulting in a significantly higher $R_{Hc:L}$.

Molecular rearrangement was observed in ITZ-TPGS-CLT nanoparticles during storage, resulting in an even higher surface hydrophilicity of the nanoparticles after storage for 2 h, as suggested by a decrease in $R_{D:Hc+L}$ (from 0.035±0.0054 to 0.008±0.00017; $p = 0.013$) and increases in both $R_{Hc:L}$ (from 15.00±1.56 to 43.31±3.39; $p = 0.0013$) and $R_{Hc:D+L}$ (from 9.57±0.19 to 32.04±2.02; $p = 0.0025$). CLT appeared to expedite the rearrangement process of TPGS during storage, since ITZ-TPGS-CLT nanoparticles ($R_{D:Hc+L}$= 0.008±0.00017 ; $R_{Hc:L}$= 43.31±3.39) showed a smaller $R_{D:Hc+L}$ ($p = 0.00038$) and a larger $R_{Hc:L}$ ($p = 0.0027$) compared with ITZ-TPGS nanoparticles after storage ($R_{D:Hc+L}$= 0.031±0.00093 ; $R_{Hc:L}$= 12.24±0.79). The extremely high relative atomic concentration of $C_{(286-288)}$ of the hydrophilic parts of TPGS and CLT after storage (93.28 ± 0.62%) (Fig. 6b) showed that the surface of ITZ-TPGS-CLT nanoparticles was nearly fully coated by hydrophiles, giving rise to the most stable formulation.

3.6. Morphology and phase imaging analysis of nanoparticles with CLT

Quantitative analysis of hydrophiles on the surface of ITZ-TPGS-CLT nanoparticles by XPS is limited by the fact that the peaks for the hydrophilic parts of TPGS and CLT need to be grouped together for the analysis. It was speculated that TPGS should be present on ITZ-TPGS-CLT nanoparticle surface in a much larger quantity than CLT in order to achieve better particle stability. To verify this speculation, the ITZ-TPGS-CLT nanoparticles were subjected to phase imaging analysis using AFM. The hydrophilic PEG groups in TPGS will acquire a darker coloration in phase imaging analysis if the local concentration of PEG moieties is sufficiently high [29].

As shown in Fig. 7, ITZ-TPGS-CLT nanoparticles were roughly spherical in shape. Their observed particle size in AFM was in good agreement with that measured by DLS particle sizing (88.4±1.75nm). No dark coating was observed in freshly

prepared nanoparticles of ITZ-TPGS-CLT, indicating that such nanoparticle preparation was not fully coated by the PEG of TPGS initially. In the presence of CLT, ITZ-TPGS-CLT nanoparticles stored for two hours showed thick dark coatings (Fig. 7b). This confirms that the extremely high relative atomic concentration of $C_{(286\text{-}288)}$ of the hydrophilic parts of TPGS and CLT on ITZ-TPGS-CLT nanoparticles after storage was dominantly contributed by the PEG of TPGS. ITZ-TPGS-CLT nanoparticles were covered mostly by TPGS but not CLT. Based on the XPS and AFM results, CLT improved the particle stability through indirect facilitation of the initial re-orientation and rearrangement of TPGS, as illustrated in Fig. 8.

3.7. Physical interaction between CLT and AS/ITZ

Being hydrophobic, CLT is expected to exhibit hydrophobic interaction with ITZ and the hydrophobic part of AS. Nevertheless, it is possible that CLT can develop additional interactions with the latter by creating new bonds (e.g., hydrogen bond and dipole-dipole bond through polar groups). Since ITZ as well as the hydrophilic and hydrophobic parts of TPGS co-existed on the particle surface of freshly prepared ITZ-TPGS-CLT nanoparticles (as shown by non-zero values for their corresponding relative atomic concentrations in Fig. 6a), any changes in the chemical environment of various types of bonding could also be visualized in XPS spectrum [30]. As depicted in Fig. S3 in supplementary information, no new characteristic peak appeared and the binding energies of the formulations with and without CLT remained essentially the same for all analyzed elements, showing that no new chemical bond was formed by CLT. FTIR data also supported such an inference. Since ITZ-CLT nanoparticles (ITZ:CLT = 1:0.2 w/w) were highly unstable and showed extensive precipitation within seconds, the visible precipitates could be readily collected for analysis. This procedure cannot be applied to the TPGS-CLT nanoparticles which have excellent stability (since no precipitate was discernable for at least 1 month). Hence, rotary evaporation was used instead to produce a TPGS-CLT solid dispersion for analysis. No peak shift was observed for the ITZ-CLT precipitates and the TPGS-CLT solid dispersion (see Fig. S4 in supplementary data). Thus, it can be concluded that CLT interacts with ITZ and TPGS solely through hydrophobic interaction.

3.8. Universal stability-enhancing effect of CLT

It has been shown that CLT is capable of improving the stability of ITZ-TPGS nanoparticles by facilitating the re-orientation and expediting the rearrangement of AS molecules during storage. To determine whether CLT could also exert similar stability-enhancing effects on nanoparticles of other drugs generated by FNP, nanosuspensions of two more hydrophobic azole drugs, ketoconazole (KTZ) (log P = 3.84) and terconazole (TZ) (log P = 3.51), with TPGS and CLT as stabilizers were prepared using basically the same protocol as described for ITZ in Section 2.2.

Fig. 9 shows that both KTZ-TPGS and TZ-TPGS nanosuspensions became much more stable after the incorporation of CLT, suggesting that similar orientation problem of AS exists in these two nanoparticle preparations, which can also be circumvented by incorporation of CLT. As with the ITZ-TPGS-CLT nanoparticles, the stability enhancement in both KTZ-TPGS-CLT and TZ-TPGS-CLT systems can also be explained with reference to the solubility parameter values of the various hydrophobic components involved. For instance, KTZ has a solubility parameter value of 24.8 [31]. Therefore, the absolute value of solubility parameter difference between CLT and vitamin E succinate would be 0.5 $(MJ/m^3)^{1/2}$, which is much smaller than that between KTZ and vitamin E succinate [5.8 $(MJ/m^3)^{1/2}$].

4. Conclusions

The involvement of a hydrophobic co-stabilizer (CLT) which is more comparable than the chosen drug (ITZ) to the hydrophobic segment of ASs (TPGS and PEG-PLA) in terms of solubility parameter values was found to effectively reduce the initial particle size and enhance the short-term storage stability of ITZ nanoparticles. XPS analysis demonstrated that incorporation of CLT improved the molecular orientation of ASs on freshly prepared ITZ nanoparticles. Additionally, the molecular rearrangement process of ASs during storage was expedited in the presence of CLT, leading to a higher PEG surface coverage for the nanoparticles and thus better stability. Detection by AFM of the dark coating on ITZ-TPGS-CLT nanoparticles after 2 hours of storage further substantiated that the nanoparticles were virtually covered with PEG. The observed enhancement of particle stability by CLT is ascribable to its stronger affinity with the hydrophobic segment of the AS than with ITZ. Since the stability-enhancing effect of CLT is solely based on hydrophobic interaction, it should not be specific to particular ASs or drugs. In other words, addition of any hydrophobic co-

stabilizer with a solubility parameter value close to that of the hydrophobic segment of AS should also be equally effective for co-stabilizing FNP-generated nanoparticles of the same drug with the AS.

Acknowledgement

We gratefully acknowledge financial support from the Chinese University of Hong Kong (Postgraduate Studentship for KYW) and the University of Hong Kong (Project number: 204600519). We also thank Prof. Robert K. Prud'homme (Department of Chemical and Biological Engineering, Princeton University) for assistance with refabrication of an MIVM for the current study at CUHK.

Supporting Information

The Supporting Information is available free of charge on the ACS Publications website at DOI:

Zeta potential of ITZ-AS nanoparticles with or without CLT; Classification of carbon binding energy ranges in ITZ, TPGS, PEG-PLA and CLT ; XPS spectrum on carbon, nitrogen, oxygen, and chlorine of freshly prepared ITZ-TPGS nanoparticles with and without CLT; FTIR spectra of ITZ-CLT precipitate and TPGS-CLT solid dispersion

The authors declare no competing financial interest.

Figures

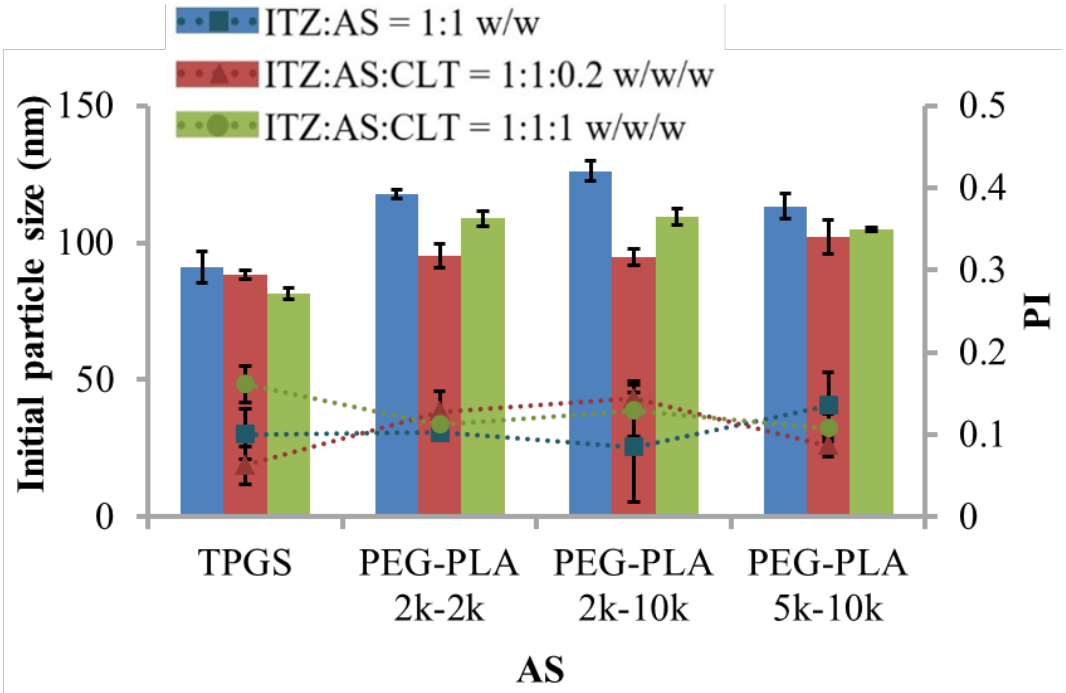

Fig. 1. Initial particle sizes (bars) and PIs (dotted lines) of ITZ-AS nanoparticles prepared with or without CLT. The PIs of all the nanoparticles produced were less than 0.2 (n = 3).

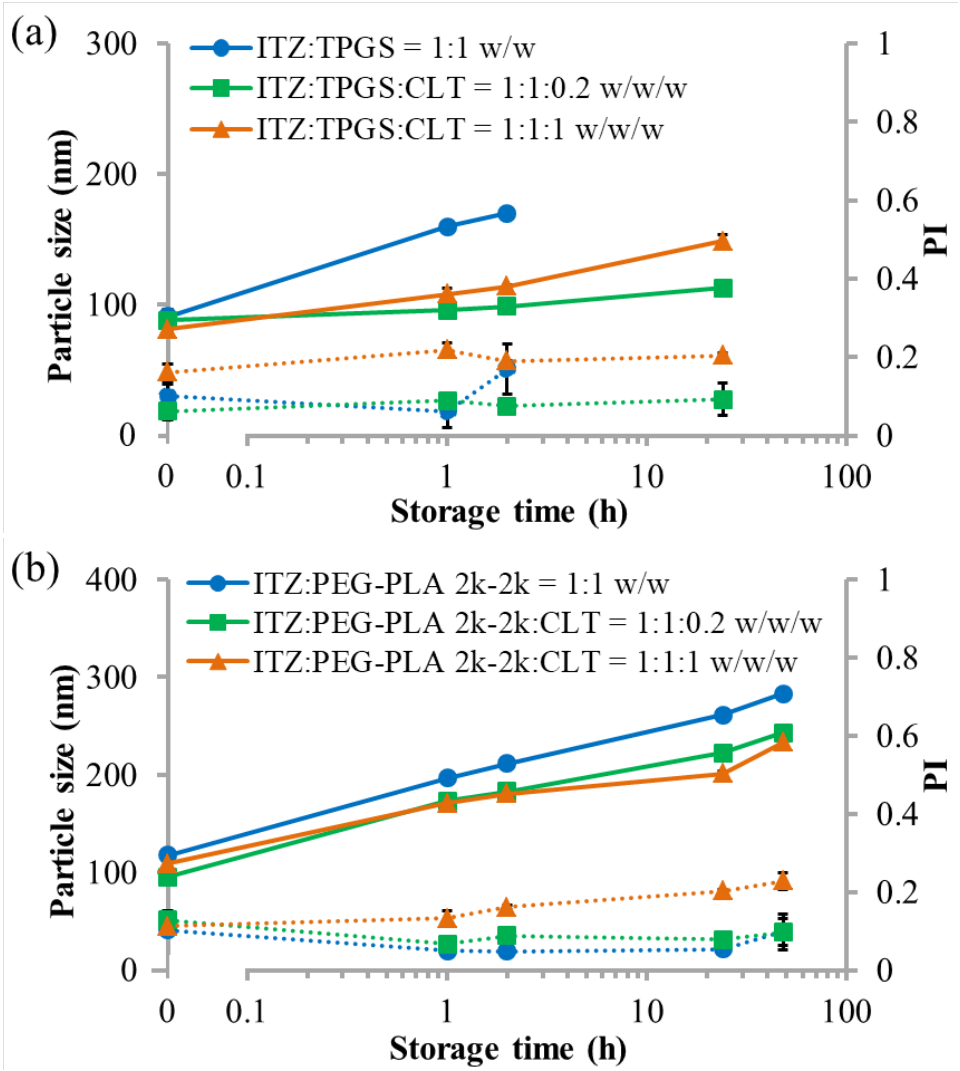
(a)
ITZ:TPGS = 1:1 w/w
ITZ:TPGS:CLT = 1:1:0.2 w/w/w
ITZ:TPGS:CLT = 1:1:1 w/w/w
Particle size (nm)
PI
Storage time (h)
0
100
200
300
0.2
0.4
0.6
0.8
1
0.1
10
(b)
ITZ:PEG-PLA 2k-2k = 1:1 w/w
ITZ:PEG-PLA 2k-2k:CLT = 1:1:0.2 w/w/w
ITZ:PEG-PLA 2k-2k:CLT = 1:1:1 w/w/w
Particle size (nm)
PI
Storage time (h)
400

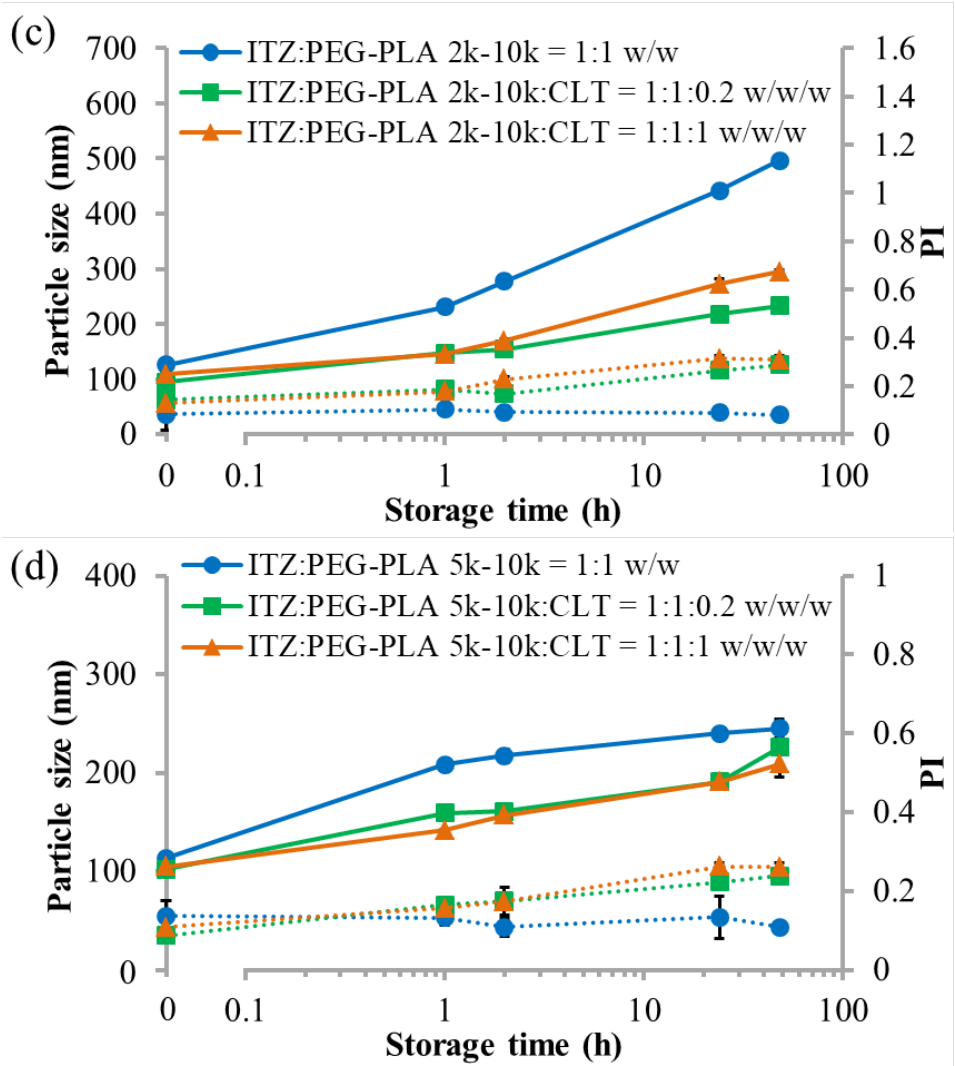

Fig. 2. Influence of CLT on the stability in term of particle sizes (solid lines) and PIs (dotted lines) of ITZ nanosuspensions prepared with various

ASs when stored at 25°C: (a) TPGS, (b) PEG-PLA 2k-2k, (c) PEG-PLA 2k-10k, and (d) PEG-PLA 5k-10k (n = 3).

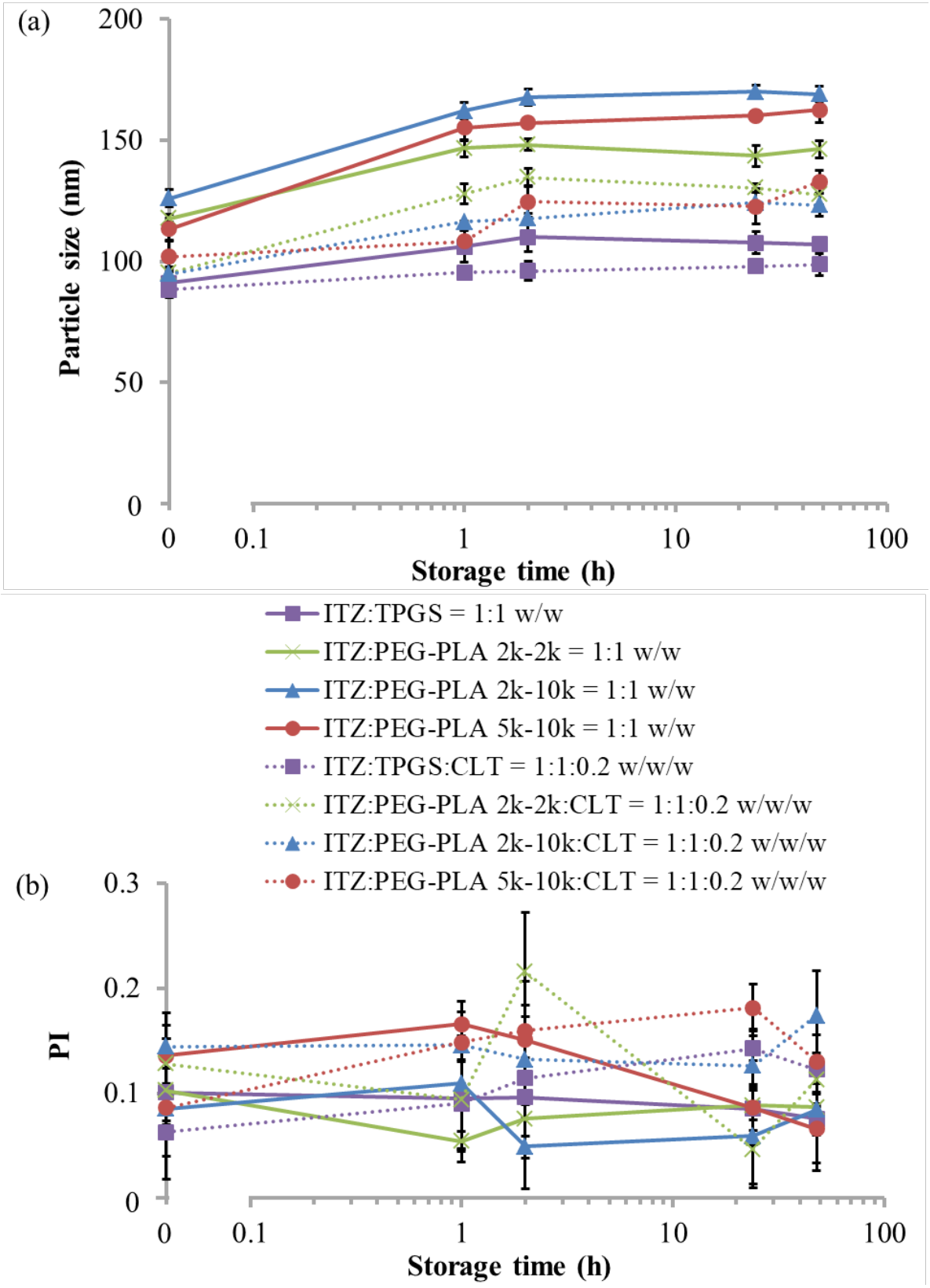

Fig. 3. Stability profiles (a) in term of particle sizes and (b) PIs of ITZ-AS nanoparticles without CLT (solid lines) and with CLT (dotted lines) when stored at 4°C (n = 3).

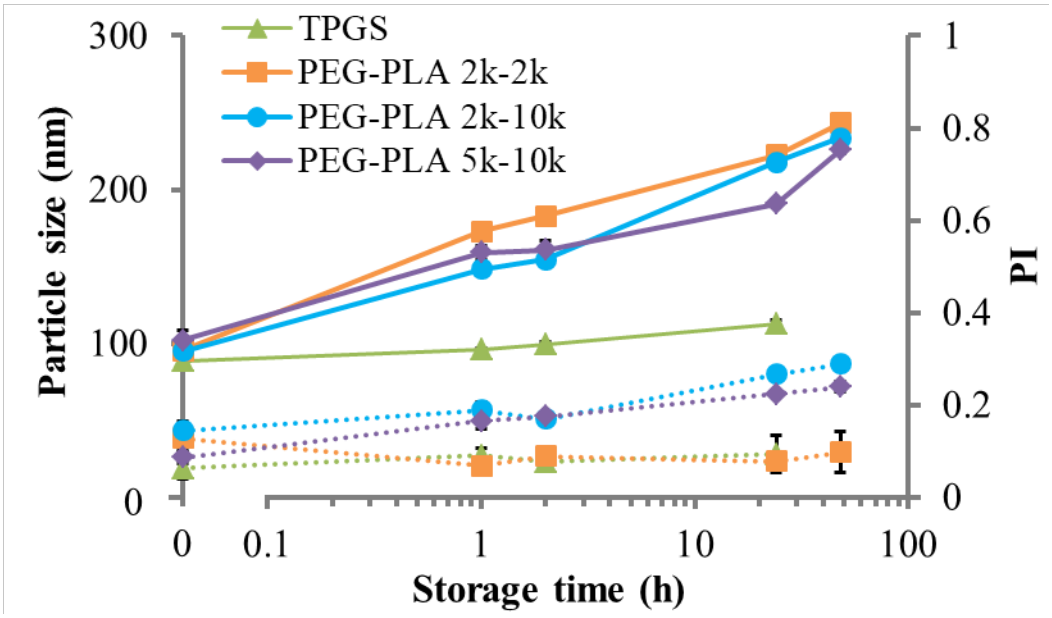

Fig. 4. Stability profiles (a) in term of particle size and (b) PIs of ITZ-AS-CLT nanoparticles (ITZ:AS:CLT = 1:1:0.2 w/w/w) when stored at 25°C (n = 3).

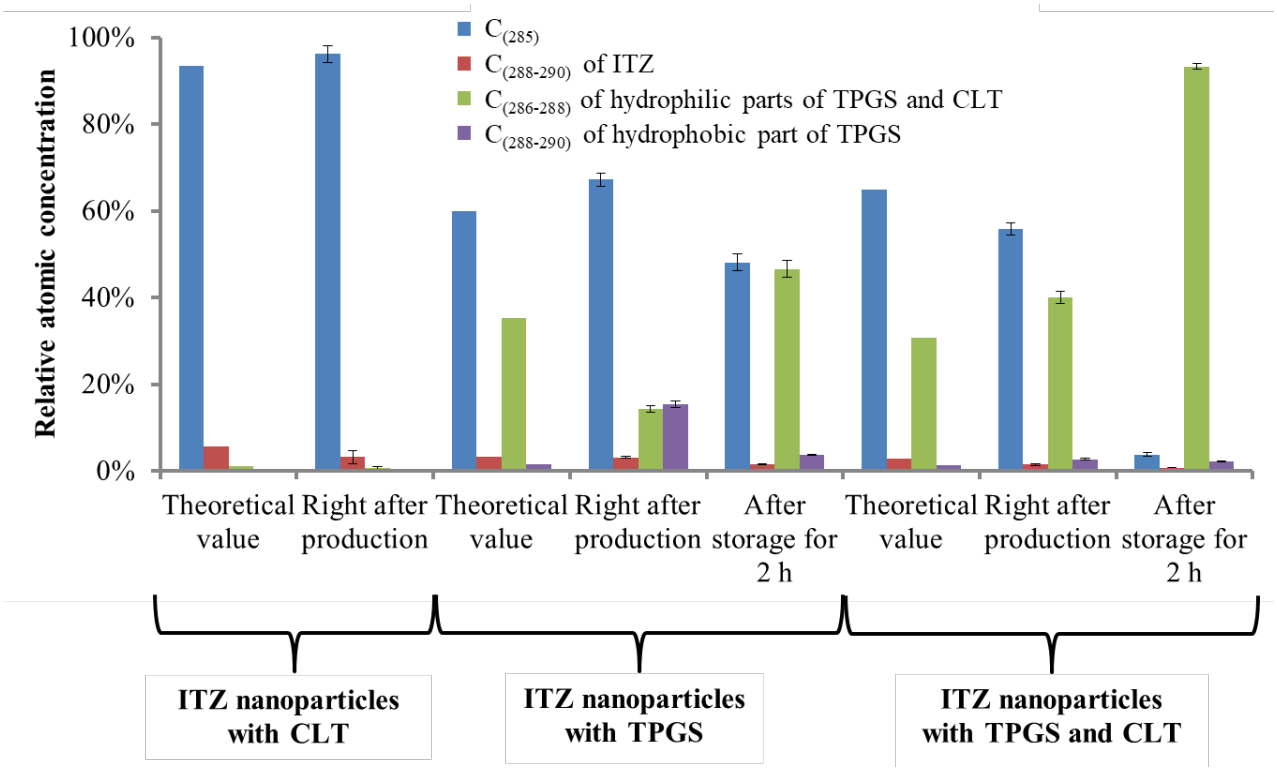

Fig. 5. Relative atomic concentrations of different carbon ranges of ITZ nanoparticles with or without TPGS and/or CLT (n = 3).

(a)

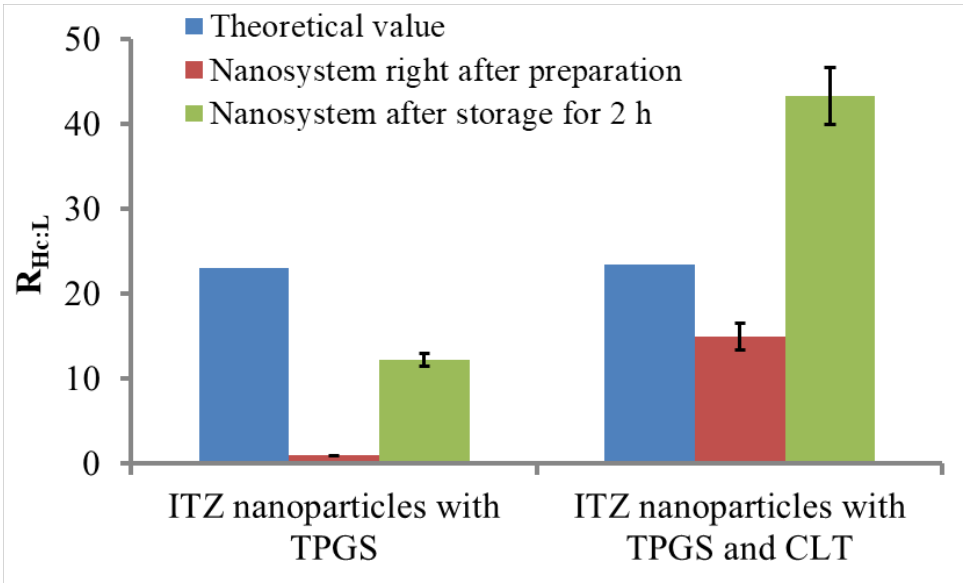
Theoretical value
Nanosystem right after preparation
Nanosystem after storage for 2 h
$R_{Hc:L}$
50
40
30
20
10
0
ITZ nanoparticles with TPGS
ITZ nanoparticles with TPGS and CLT

(b)

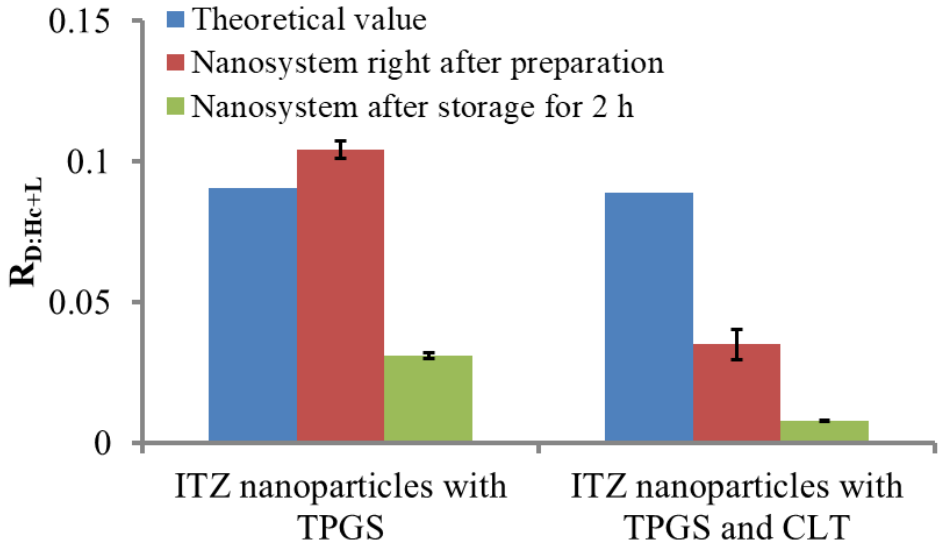
Theoretical value
Nanosystem right after preparation
Nanosystem after storage for 2 h
$R_{D:Hc+L}$
0.15
0.1
0.05
0
ITZ nanoparticles with TPGS
ITZ nanoparticles with TPGS and CLT

(c)

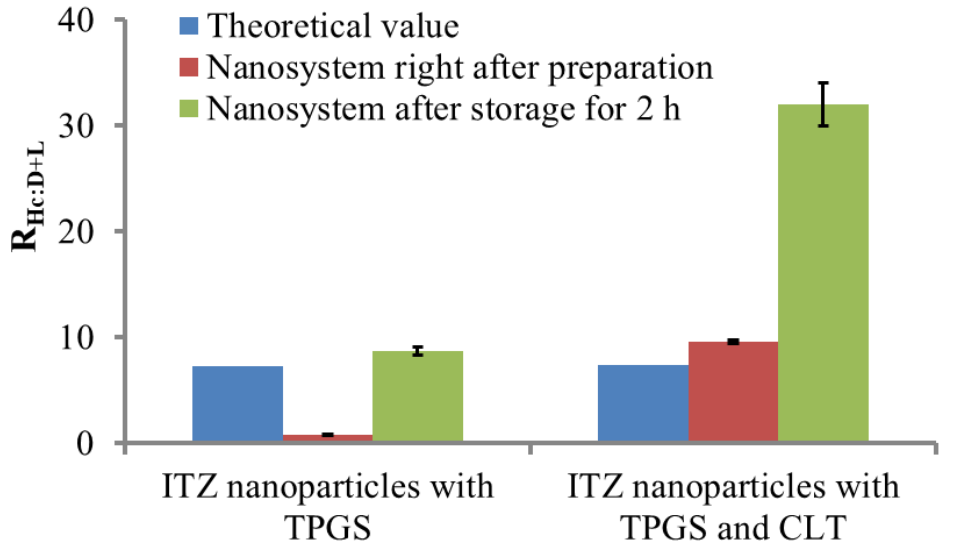
Theoretical value
Nanosystem right after preparation
Nanosystem after storage for 2 h
$R_{Hc:D+L}$
40
30
20
10
0
ITZ nanoparticles with TPGS
ITZ nanoparticles with TPGS and CLT

Fig. 6. Atomic concentration ratios of (a) $C_{(286\text{-}288)}$ of the hydrophilic parts of TPGS and CLT to $C_{(288\text{-}290)}$ of the hydrophobic part of TPGS ($R_{Hc:L}$; n=3); (b) $C_{(288\text{-}290)}$ of ITZ to $C_{(286\text{-}288)}$ of the hydrophilic parts of TPGS and CLT plus $C_{(288\text{-}290)}$ of the hydrophobic part of TPGS ($R_{D:Hc+L}$; n=3); and (c) $C_{(286\text{-}288)}$ of the hydrophilic parts of TPGS and CLT to $C_{(288\text{-}290)}$ of ITZ plus $C_{(288\text{-}290)}$ of the hydrophobic part of TPGS ($R_{Hc:D+L}$; n=3).

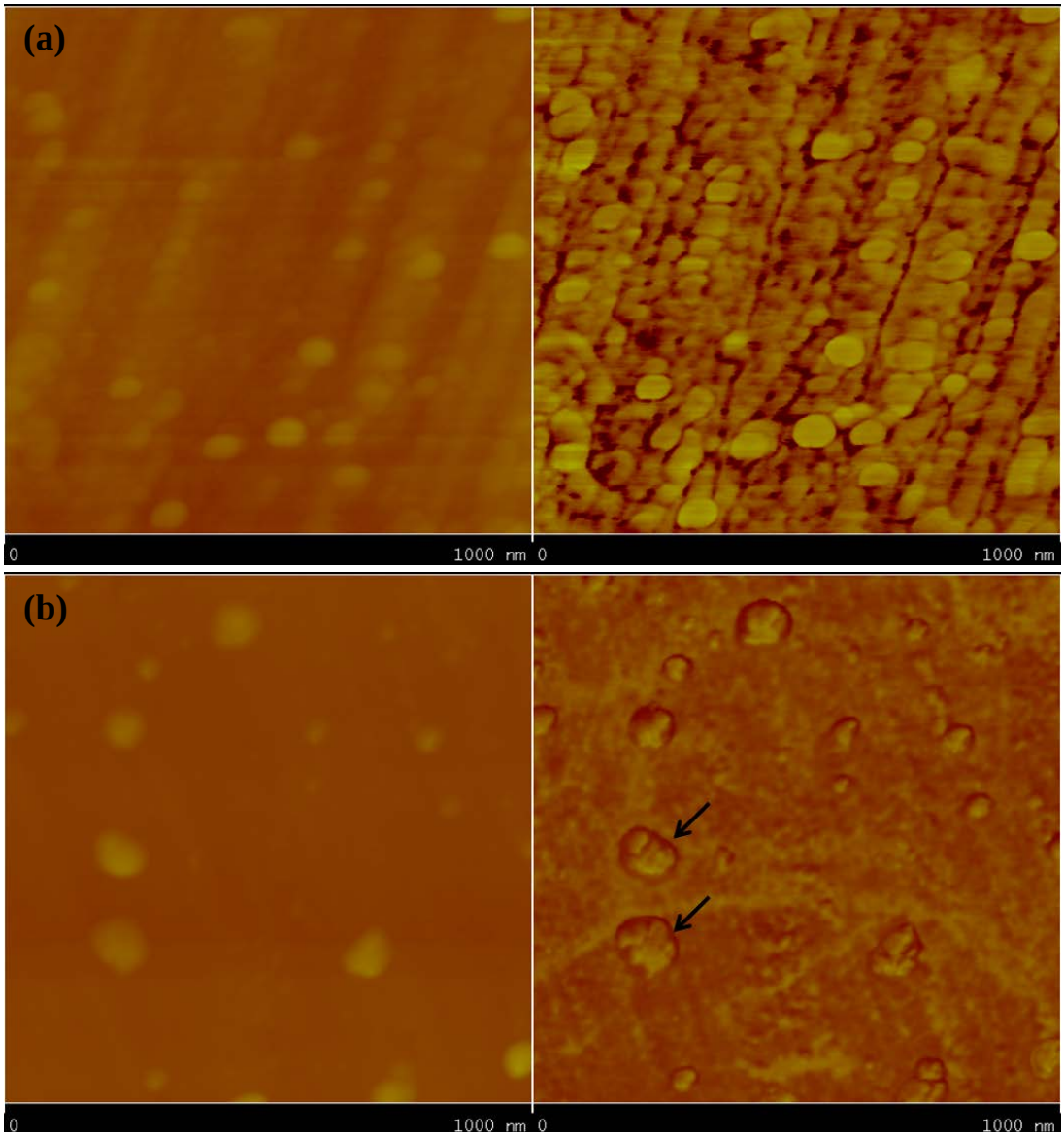

Fig. 7. Topographic image (left) and phase image (right) of ITZ-TPGS-CLT nanoparticles (a) right after production and (b) after storage for 2 h (dark coating of particles was indicated by arrows).

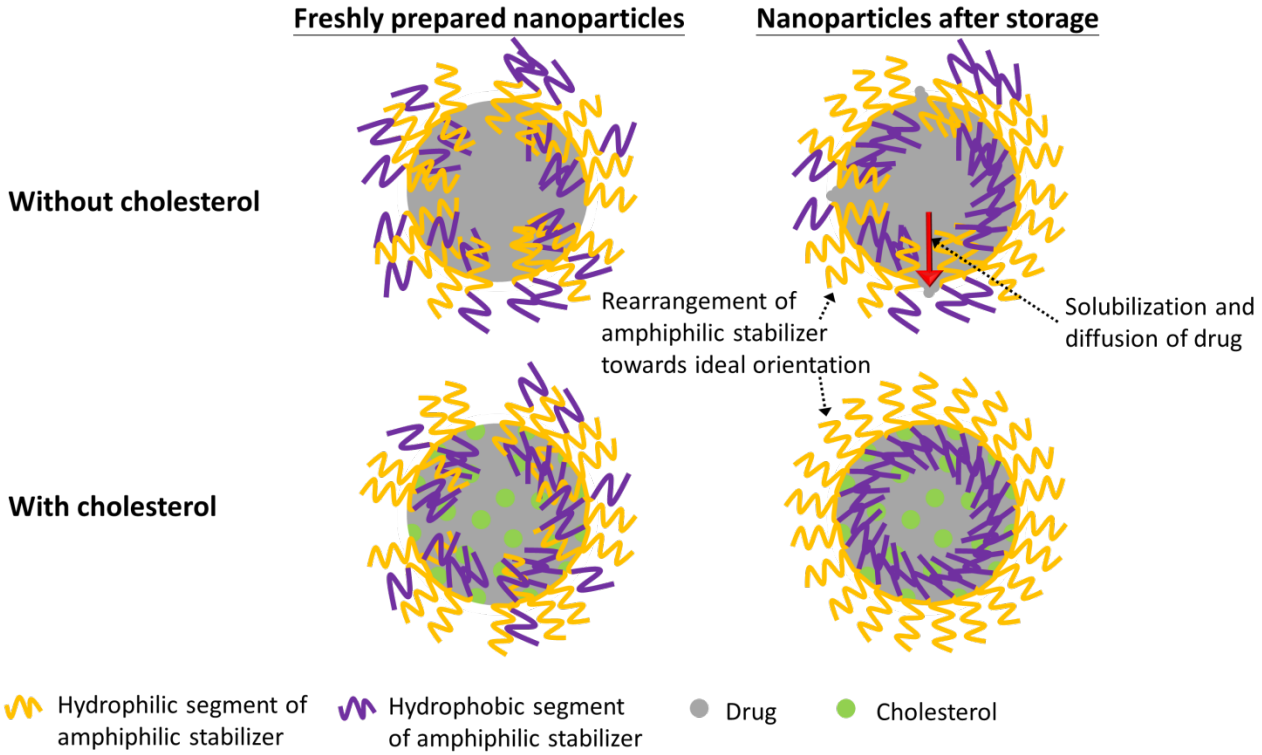

Fig. 8. A schematic diagram illustrating that CLT indirectly facilitates initial orientation and rearrangement of AS molecules during short-term storage.

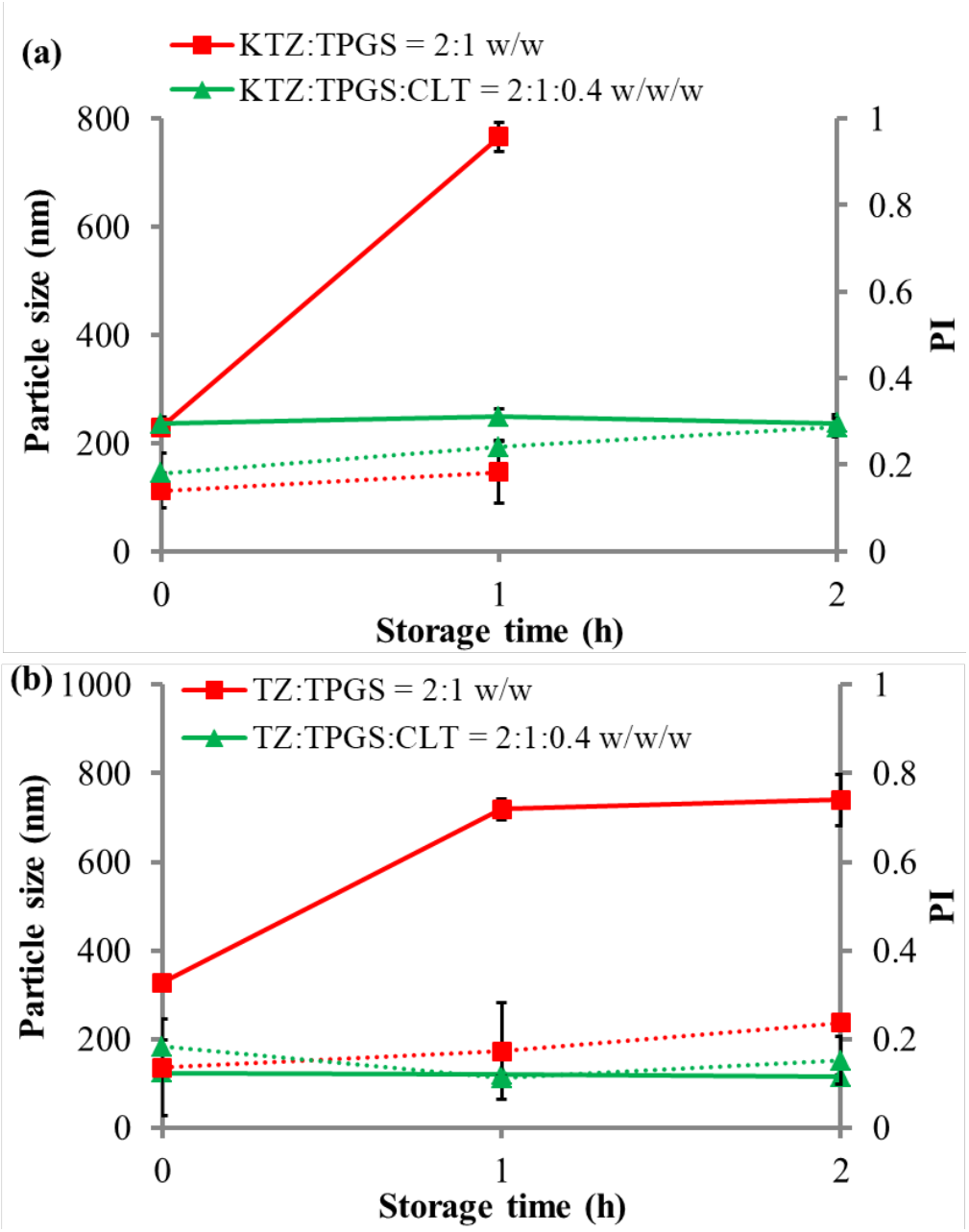

Fig. 9. Stability profiles in term of particle size (solid lines) and PIs (dotted lines) of (a) KTZ-TPGS and (b) TZ-TPGS nanoparticles with and without CLT (n = 3).

References

1. Liversidge, G. G.; Cundy, K. C., Particle-Size Reduction for Improvement of Oral Bioavailability of Hydrophobic Drugs .1. Absolute Oral Bioavailability of Nanocrystalline Danazol in Beagle Dogs. *Int. J. Pharm.* **1995,** *125*, 91-97.

2. Ganta, S.; Paxton, J. W.; Baguley, B. C.; Garg, S., Formulation and pharmacokinetic evaluation of an asulacrine nanocrystalline suspension for intravenous delivery. *Int. J. Pharm.* **2009,** *367*, 179-186.

3. Zhang, Q.; Shen, Z. C.; Nagai, T., Prolonged hypoglycemic effect of insulin-loaded polybutylcyanoacrylate nanoparticles after pulmonary administration to normal rats. *Int. J. Pharm.* **2001,** *218*, 75-80.

4. Italia, J. L.; Bhatt, D. K.; Bhardwaj, V.; Tikoo, K.; Kumar, M. N. V. R., PLGA nanoparticles for oral delivery of cyclosporine: Nephrotoxicity and pharmacokinetic studies in comparison to Sandimmune Neoral (R). *J. Controlled Release* **2007,** *119*, 197-206.
5. Allen, T. M.; Cullis, P. R., Drug delivery systems: Entering the mainstream. *Science* **2004,** *303*, 1818-1822.
6. Fernandes, C.; Soni, U.; Patravale, V., Nano-interventions for neurodegenerative disorders. *Pharmacol. Res.* **2010,** *62*, 166-78.
7. Chow, S. F.; Sun, C. C.; Chow, A. H. L., Assessment of the relative performance of a confined impinging jets mixer and a multi-inlet vortex mixer for curcumin nanoparticle production. *Eur. J. Pharm. Biopharm.* **2014,** *88*, 462-471.
8. Liu, Y.; Cheng, C. Y.; Liu, Y.; Prud'homme, R. K.; Fox, R. O., Mixing in a multi-inlet vortex mixer (MIVM) for flash nano-precipitation. *Chem. Eng. Sci.* **2008,** *63*, 2829-2842.
9. Johnson, B. K.; Prud'homme, R. K., Chemical processing and micromixing in confined impinging jets. *AIChE J.* **2003,** *49*, 2264-2282.
10. Chow, S. F.; Wan, K. Y.; Cheng, K. K.; Wong, K. W.; Sun, C. C.; Baum, L.; Chow, A. H. L., Development of highly stabilized curcumin nanoparticles by flash nanoprecipitation and lyophilization. *Eur. J. Pharm. Biopharm.* **2015,** *94*, 436-449.
11. Zhu, Z. X.; Anacker, J. L.; Ji, S. X.; Hoye, T. R.; Macosko, C. W.; Prud'homme, R. K., Formation of block copolymer-protected nanoparticles via reactive impingement mixing. *Langmuir* **2007,** *23*, 10499-10504.
12. Zhu, Z. X.; Margulis-Goshen, K.; Magdassi, S.; Talmon, Y.; Macosko, C. W., Polyelectrolyte Stabilized Drug Nanoparticles via Flash Nanoprecipitation: A Model Study With beta-Carotene. *J. Pharm. Sci.* **2010,** *99*, 4295-4306.
13. Liu, Y.; Tong, Z.; Prud'homme, R. K., Stabilized polymeric nanoparticles for controlled and efficient release of bifenthrin. *Pest Manage. Sci.* **2008,** *64*, 808-12.
14. Zhang, Y. Y.; Feng, J.; McManus, S. A.; Lu, H. D.; Ristroph, K. D.; Cho, E. J.; Dobrijevic, E. L.; Chan, H. K.; Prud'homme, R. K., Design and Solidification of Fast-Releasing Clofazimine Nanoparticles for Treatment of Cryptosporidiosis. *Mol. Pharmaceutics* **2017,** *14*, 3480-3488.
15. Zhu, Z. X., Flash Nanoprecipitation: Prediction and Enhancement of Particle Stability via Drug Structure. *Mol. Pharmaceutics* **2014,** *11* (3), 776-786.
16. Liu, Y.; Kathan, K.; Saad, W.; Prud'homme, R. K., Ostwald ripening of beta-carotene nanoparticles. *Phys. Rev. Lett.* **2007,** *98*, 036102.
17. Zhu, Z. X., Effects of amphiphilic diblock copolymer on drug nanoparticle formation and stability. *Biomaterials* **2013,** *34*, 10238-10248.
18. Zhang, C.; Pansare, V. J.; Prud'homme, R. K.; Priestley, R. D., Flash nanoprecipitation of polystyrene nanoparticles. *Soft Matter* **2012,** *8*, 86-93.
19. Barton, A. F. M., *CRC handbook of solubility parameters and other cohesion parameters*. 2nd ed.; CRC Press: Boca Raton, 1991~~; pp 739~~.
20. Wan, K. Y.; Wong, K. W.; Chow, A. H. L.; Chow, S. F., Impact of molecular rearrangement of amphiphilic stabilizers on physical stability of itraconazole nanoparticles prepared by flash nanoprecipitation. *Int. J. Pharm.* **2018,** *542*, 221-231.
21. Vaughan, C. D., Using Solubility Parameters in Cosmetics Formulation. *J. Soc. Cosmet. Chem.* **1985,** *36*, 319-333.
22. Bellantone, R. A.; Patel, P.; Sandhu, H.; Choi, D. S.; Singhal, D.; Chokshi, H.; Malick, A. W.; Shah, N., A method to predict the equilibrium solubility of drugs in solid polymers near room temperature using thermal analysis. *J. Pharm. Sci.* **2012,** *101*, 4549-4558.

23. Hwang, J. J.; Iyer, S. N.; Li, L. S.; Claussen, R.; Harrington, D. A.; Stupp, S. I., Self-assembling biomaterials: Liquid crystal phases of cholesteryl oligo(L-lactic acid) and their interactions with cells. *Proc. Natl. Acad. Sci. U. S. A.* **2002,** *99*, 9662-9667.
24. Costanzo, R.; Depaoli, T.; Ihlo, J. E.; Hager, A. A.; Farach, H. A.; Poole, C. P.; Knight, J. M., Esr Study of Order and Dynamics in Lecithin Liposomes with High Cholesterol Content. *Spectrochim. Acta, Part A* **1994,** *50*, 203-208.
25. Dai, J.; Alwarawrah, M.; Huang, J. Y., Instability of Cholesterol Clusters in Lipid Bilayers and The Cholesterol's Umbrella Effect. *J. Phys. Chem. B* **2010,** *114*, 840-848.
26. Briggs, D., *Handbook of x-ray and ultraviolet photoelectron spectroscopy*. Heyden: London ; Philadelphia, 1977~~; p xiii, pp 398.~~
27. Jacobs, C.; Kayser, O.; Muller, R. H., Nanosuspensions as a new approach for the formulation for the poorly soluble drug tarazepide. *Int. J. Pharm.* **2000,** *196*, 161-164.
28. Miller, D. J.; Biesinger, M. C.; McIntyre, N. S., Interactions of CO2 and CO at fractional atmosphere pressures with iron and iron oxide surfaces: one possible mechanism for surface contamination? *Surf. Interface Anal.* **2002,** *33*, 299-305.
29. Essa, S.; Rabanel, J. M.; Hildgen, P., Effect of polyethylene glycol (PEG) chain organization on the physicochemical properties of poly(D, L-lactide) (PLA) based nanoparticles. *Eur. J. Pharm. Biopharm.* **2010,** *75*, 96-106.
30. Maniruzzaman, M.; Morgan, D. J.; Mendham, A. P.; Pang, J. Y.; Snowden, M. J.; Douroumis, D., Drug-polymer intermolecular interactions in hot-melt extruded solid dispersions. *Int. J. Pharm.* **2013,** *443*, 199-208.
31. Langer, M.; Holtje, M.; Urbanetz, N. A.; Brandt, B.; Holtje, H. D.; Lippold, B. C., Investigations on the predictability of the formation of glassy solid solutions of drugs in sugar alcohols. *Int. J. Pharm.* **2003,** *252*, 167-79.

Interplay between Amphiphilic Stabilizers and Cholesterol in the Stabilization of Itraconazole Nanoparticles Prepared by Flash Nanoprecipitation

Ka Yee Wan[1], Si Nga Wong[2], Ka Wai Wong[3], Shing Fung Chow[2,*], Albert Hee Lum Chow[1,*#]

TOC graphic:

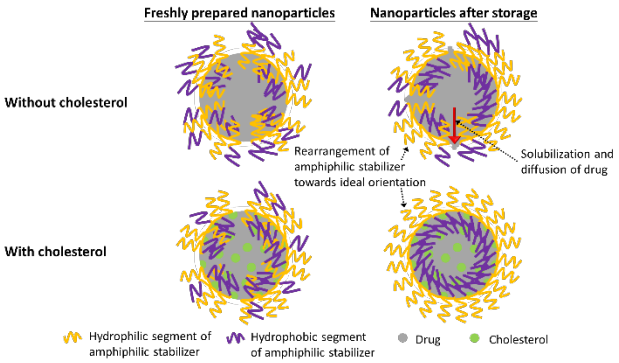

Synopsis:

Physical instability associated with non-equilibrium molecular orientation of amphiphilic stabilizers (ASs) in nanoparticles remains a hurdle in Flash Nanoprecipitation. We herein report incorporation of a co-stabilizer with solubility parameter value that is closer to the hydrophobic tail of AS than to that of drug could facilitate a stronger and more timely surface anchorage of the AS hydrophobic moieties, thereby promoting the rearrangement of AS molecules towards stable micelle-like structure.

Supporting Information

Interplay between Amphiphilic Stabilizers and Cholesterol in the Stabilization of Itraconazole Nanoparticles Prepared by Flash Nanoprecipitation

Ka Yee Wan[1], Si Nga Wong[2], Ka Wai Wong[3], Shing Fung Chow[2,*], Albert Hee Lum Chow[1,*#]

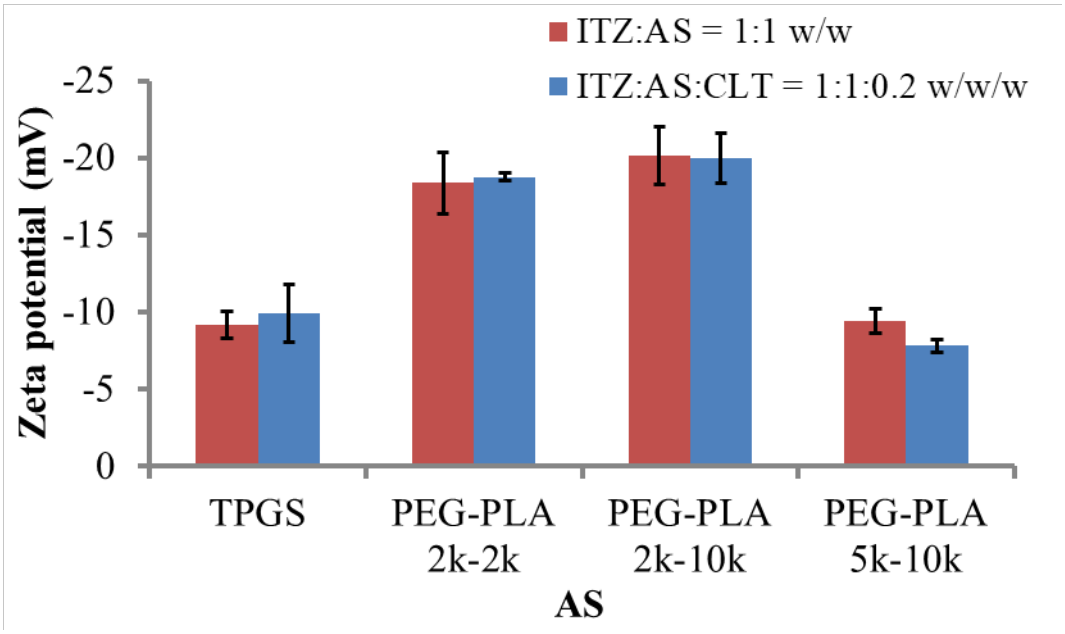

Fig. S1. Zeta potential of ITZ-AS nanoparticles with or without CLT (n = 3).

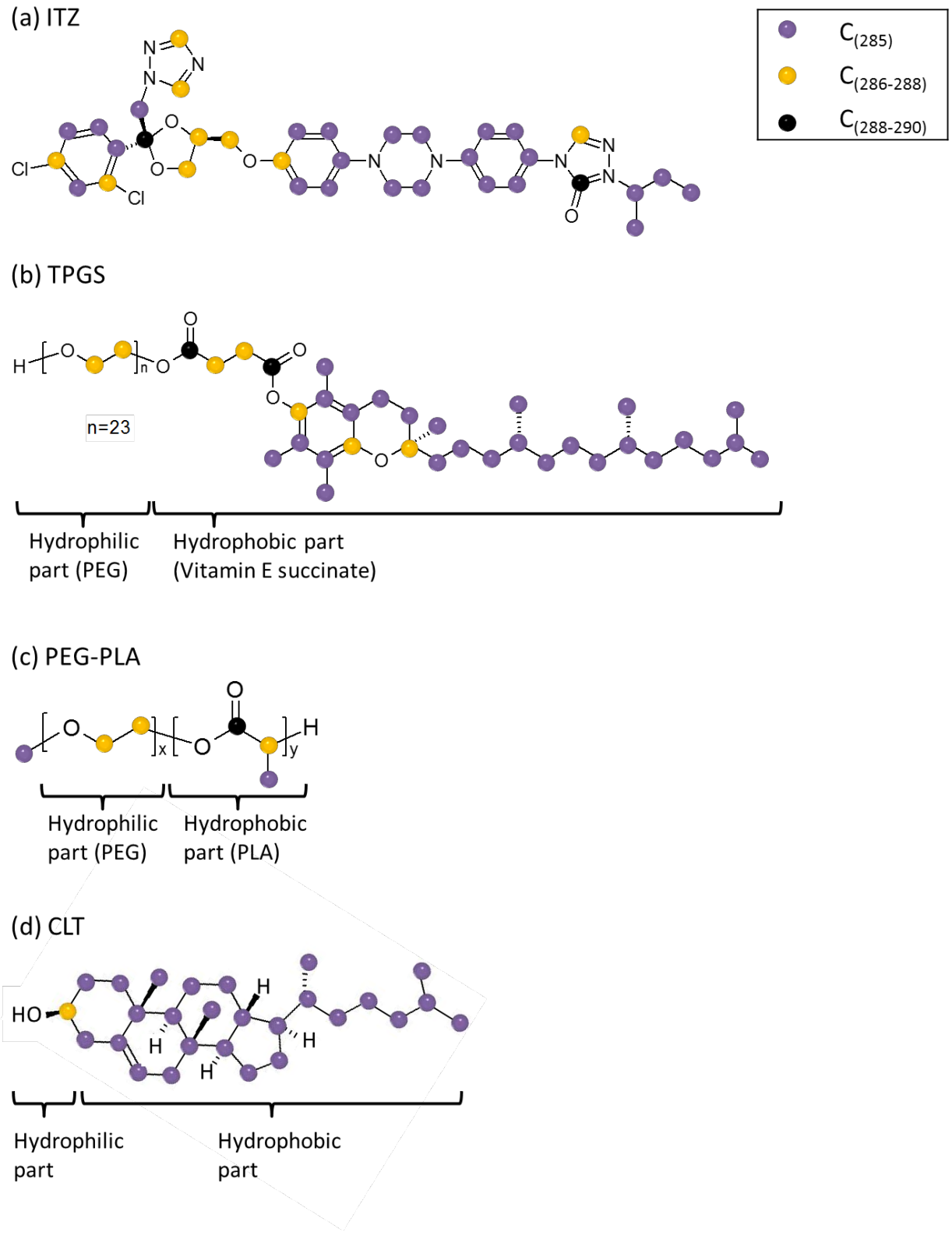

Fig. S2. Classification of carbon binding energy ranges in ITZ, TPGS, PEG-PLA and CLT (modified from reference 20).

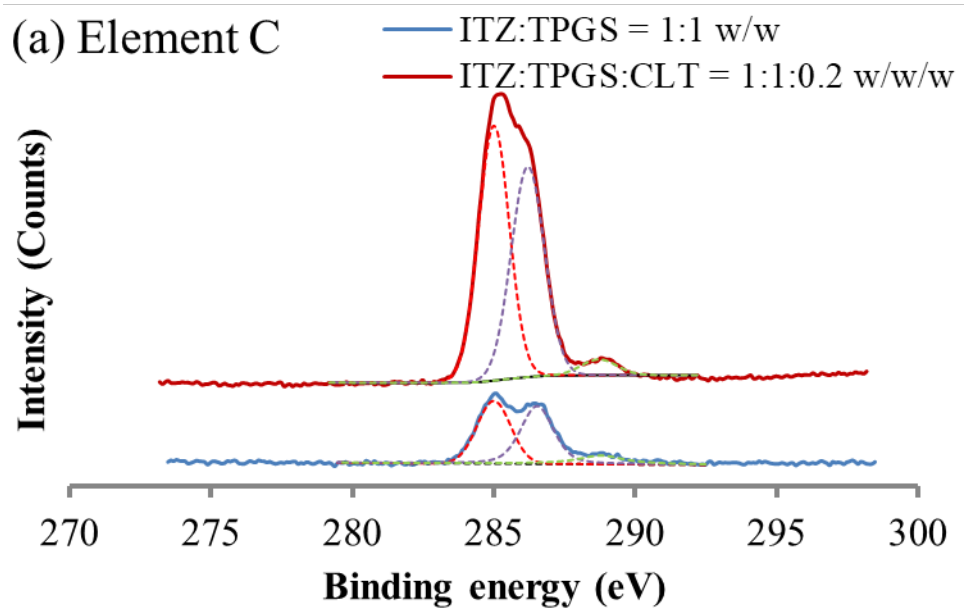
(a) Element C
ITZ:TPGS = 1:1 w/w
ITZ:TPGS:CLT = 1:1:0.2 w/w/w
Intensity (Counts)
270
275
280
285
290
295
300
Binding energy (eV)

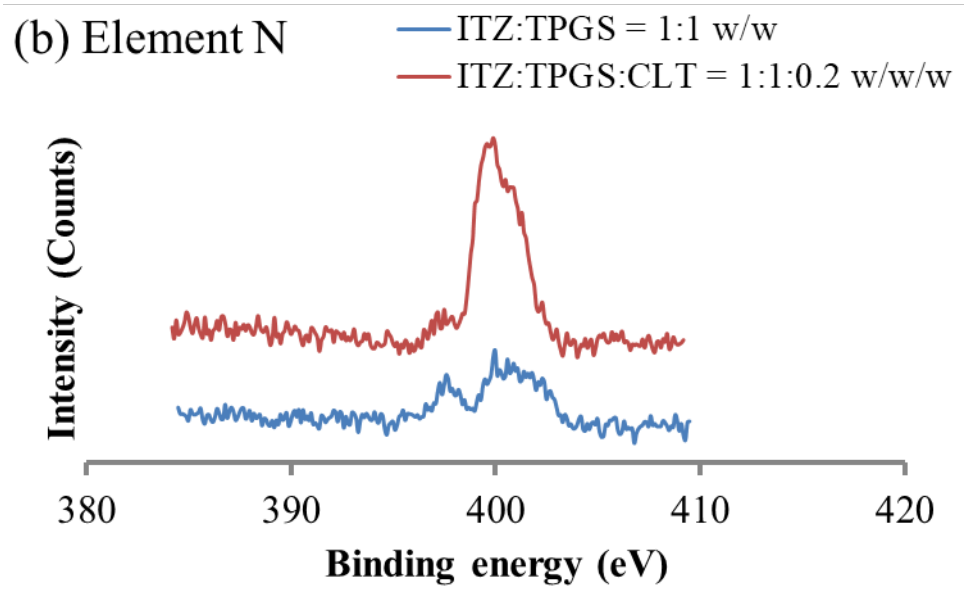
(b) Element N
ITZ:TPGS = 1:1 w/w
ITZ:TPGS:CLT = 1:1:0.2 w/w/w
Intensity (Counts)
380
390
400
410
420
Binding energy (eV)

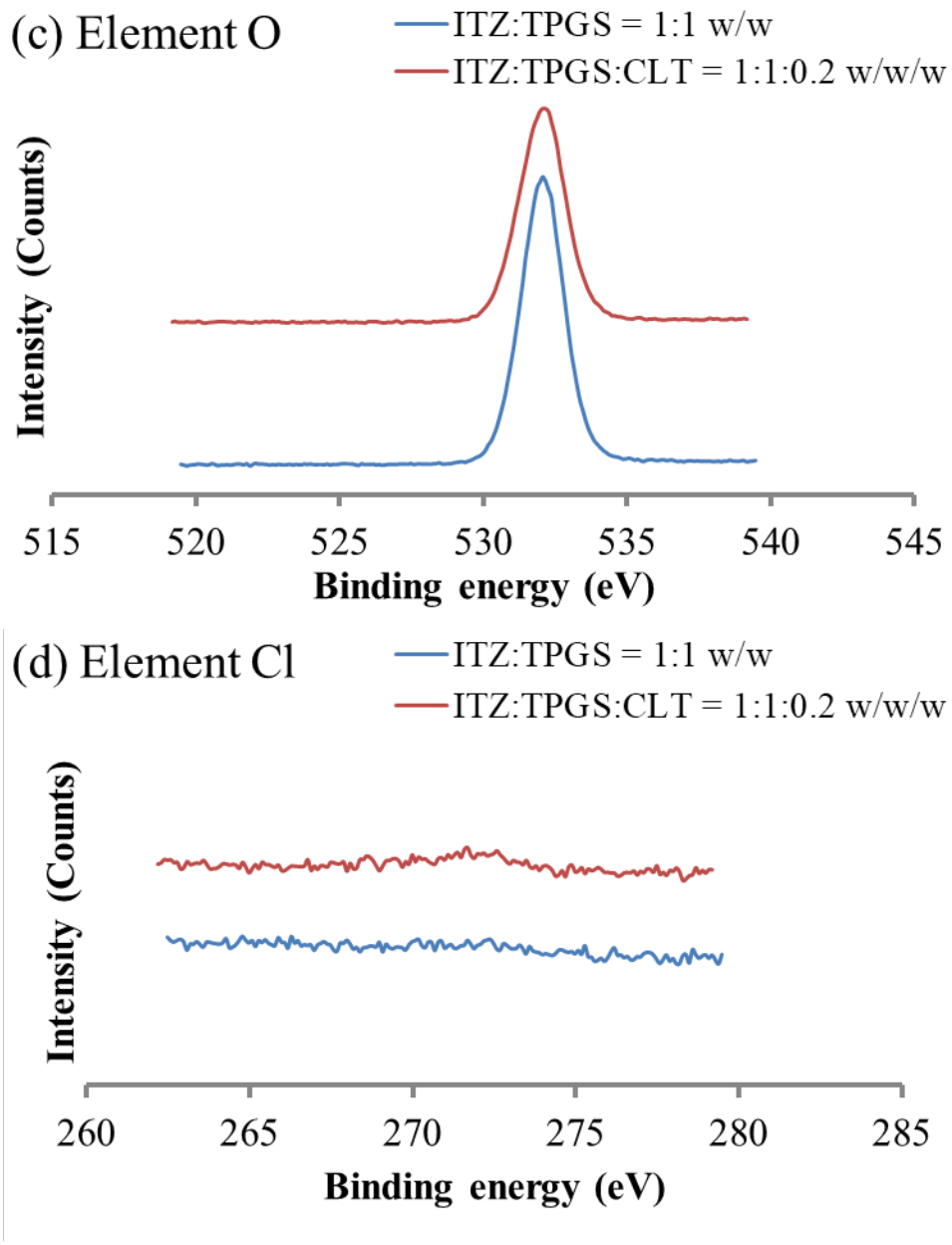

Fig. S3. XPS peaks of element (a) carbon (dotted lines showing peak deconvolution), (b) nitrogen, (c) oxygen, and (d) chlorine of freshly prepared ITZ-TPGS nanoparticles with and without CLT.

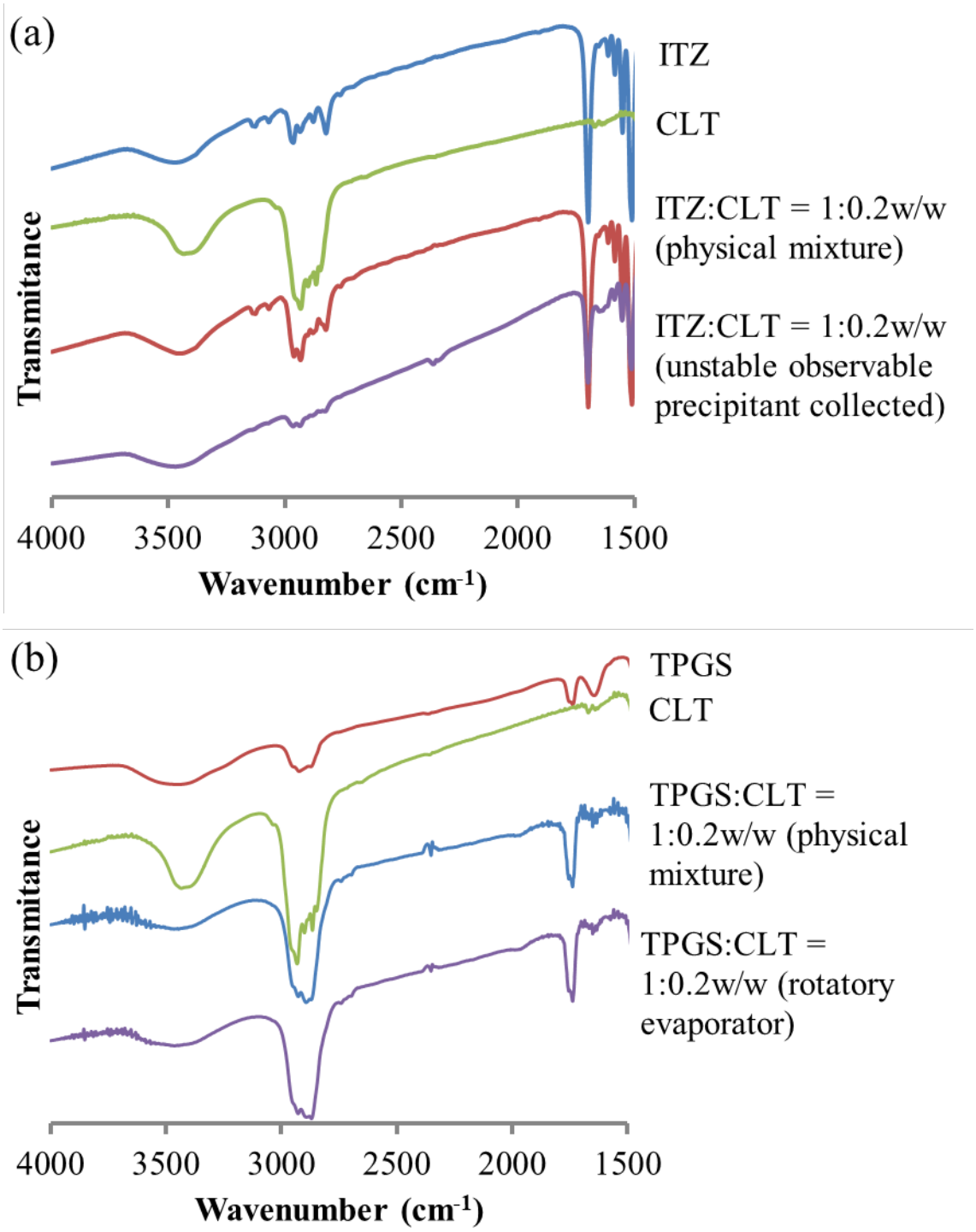

Fig. S4. FTIR spectra of (a) ITZ-CLT precipitate and (b) TPGS-CLT solid dispersion.